FGF2 gene transfer restores hippocampal functions in mouse models of Alzheimer's disease and has therapeutic implications for neurocognitive disorders

Tomomi Kiyota[a], Kaitlin L. Ingraham[b], Michael T. Jacobsen[a], Huangui Xiong[a], and Tsuneya Ikezu[a,b,1]

[a]Departments of Pharmacology and Experimental Neuroscience, University of Nebraska Medical Center, Omaha, NE 68198; and [b]Laboratory of Molecular NeuroTherapeutics, Departments of Pharmacology and Experimental Therapeutics and Neurology, and Alzheimer's Disease Center, Boston University School of Medicine, Boston, MA 02118

Edited* by Susan E. Leeman, Boston University School of Medicine, Boston, MA, and approved October 12, 2011 (received for review February 11, 2011)

The adult hippocampus plays a central role in memory formation, synaptic plasticity, and neurogenesis. The subgranular zone of the dentate gyrus contains neural progenitor cells with self-renewal and multilineage potency. Transgene expression of familial Alzheimer's disease-linked mutants of β-amyloid precursor protein (APP) and presenilin-1 leads to a significant inhibition of neurogenesis, which is potentially linked to age-dependent memory loss. To investigate the effect of neurogenesis on cognitive function in a relevant disease model, FGF2 gene is delivered bilaterally to the hippocampi of APP+presenilin-1 bigenic mice via an adenoassociated virus serotype 2/1 hybrid (AAV2/1-FGF2). Animals injected with AAV2/1-FGF2 at a pre- or postsymptomatic stage show significantly improved spatial learning in the radial arm water maze test. A neuropathological investigation demonstrates that AAV2/1-FGF2 injection enhances the number of doublecortin, BrdU/NeuN, and c-fos–positive cells in the dentate gyrus, and the clearance of fibrillar amyloid-β peptide (Aβ) in the hippocampus. AAV2/1-FGF2 injection also enhances long-term potentiation in another APP mouse model (J20) compared with control AAV2/1-GFP–injected littermates. An in vitro study confirmed the enhanced neurogenesis of mouse neural stem cells by direct AAV2/1-FGF2 infection in an Aβ oligomer-sensitive manner. Further, FGF2 enhances Aβ phagocytosis in primary cultured microglia, and reduces Aβ production from primary cultured neurons after AAV2/1-FGF2 infection. Thus, our data indicate that virus-mediated FGF2 gene delivery has potential as an alternative therapy of Alzheimer's disease and possibly other neurocognitive disorders.

fibroblast growth factor | transgenic mouse model | viral gene therapy | neurodegenerative disorders

Neurodegenerative disorders are characterized by the selective and symmetric loss of neurons in the motor, sensory, or cognitive systems (1). Alzheimer's disease (AD) is the most prevalent neurodegenerative disorder in the world (2), and is characterized by the presence of senile plaques and the formation of neurofibrillary tangles, the neurotoxicity of which is commonly believed to be responsible for synaptic failure, neuronal loss, and degeneration of the cholinergic system in patients with AD (3–5). Senile plaques are extracellular depositions of aggregated amyloid-β peptide (Aβ), although the exact pathogenesis from Aβ aggregation to neurodegeneration has not yet been fully characterized. Although active or passive Aβ immunotherapy was highly successful in amyloid clearance and improvement of spatial learning in transgenic (Tg) mouse models of AD expressing a β-amyloid precursor protein (APP) mutant (6–9), a phase II trial of Aβ vaccination therapy (AN-1792) was suspended because of the occurrence of aseptic meningoencephalitis in 6% of enrolled patients (10, 11). In addition, a recent report on a phase III trial of semagacestat, a γ-secretase inhibitor that targets the processing of APP to generate lowered amounts of Aβ, also reported unsuccessful findings (12, 13). These reports prompted us to look into alternative approaches to ameliorate AD progression, such as targeting tau aggregation, neuroinflammation, or neurogenesis.

Neurotrophic factor therapy is a promising approach for the enhancement of neuroprotection and neuronal maturation in the brain (14, 15). Nerve growth factor gene therapy represented the first neurotrophic factor testing with patients with AD in a phase I trial that reported significant reduction of cognitive decline and enhancement of glucose uptake function in the brain (14). AAV-mediated expression of nerve growth factor is also neuroprotective from axotomy for cholinergic neurons when expressed in the basal forebrain (16) or the medial septum (17), although its effect on Tg AD mouse models is unknown. Brain-derived neurotrophic factor (BDNF) also shows great potential as a neuroprotective factor when expressed in the entorhinal cortex of APP Tg mice by a recombinant lentiviral vector-mediated gene delivery system (15).

FGF2 is an established neurogenic factor of proliferation and differentiation for multipotent neural progenitors isolated from the adult mouse brain (18–21). FGF2 is a member of a large family of proteins that bind heparin and heparan sulfate and modulate the function of a wide range of cell types. In the central nervous system, FGF2 is expressed in neurogenic regions and has been implicated in the control of adult neurogenesis based on changes in proliferation and fate choice of adult neural progenitor cells (19, 22). In addition, AAV-mediated expression of FGF2 or BDNF in the retina is neuroprotective against NMDA-induced excitotoxicity and optic nerve injury (23, 24). AAV-mediated expression of FGF2 also induces survival and proliferation of transplanted adult neuronal progenitor cells when injected into the striatum compared with AAV-mediated expression of BDNF (25).

In contrast to the successful reports of FGF2 on neuroprotection and neurogenesis, the elevation of FGF2 has been documented in the AD brain, and treatment of primary cultured neurons with FGF2 has been characterized as rather inhibitory to neuronal differentiation in vitro (26, 27). These studies lead to the opinion that FGF2 up-regulation in response to neurodegeneration may be antagonistic to maturation of newly synthesized neurons and is potentially inhibitory to neuroregeneration in the AD brain, although the latter conclusion was drawn from an in vitro study (26, 27). Hence, CNS gene transfer of FGF2 has never

Author contributions: T.K., K.L.I., H.X., and T.I. designed research; T.K., K.L.I., M.T.J., and H.X. performed research; H.X. contributed new reagents/analytic tools; T.K., K.L.I., M.T.J., H.X., and T.I. analyzed data; and T.K., K.L.I., M.T.J., H.X., and T.I. wrote the paper.

The authors declare no conflict of interest.

*This Direct Submission article had a prearranged editor.

Freely available online through the PNAS open access option.

[1]To whom correspondence should be addressed. E-mail: tikezu@bu.edu.

See Author Summary on page 19469.

This article contains supporting information online at www.pnas.org/lookup/suppl/doi:10.1073/pnas.1102349108/-/DCSupplemental.

been tested in animal models of AD, and the exact role of FGF2 gene expression and its function in the AD brain remains uncharacterized. To resolve this controversy, we examined the direct effect of adenoassociated virus serotype 2/1 hybrid (AAV2/1)-mediated hippocampal gene expression of FGF2 on neurogenesis and spatial learning in APP+presenilin-1 (PS1) mice at two different time points.

Results

Long-Term Expression of FGF2 in Mouse Brain. We first tested the time course of recombinant FGF2 protein expression after stereotaxic hippocampal injection of AAV2/1-FGF2, or AAV2/1-GFP viruses as a negative control [1×10^{10} virus particles (VPs) per brain] in non-Tg mice. FGF2 expression was 1,812, 1,550, and 1,957 pg/mg at 4, 12, and 24 wk after injection, respectively, in the AAV2/1-FGF2–injected group, which is significantly higher than the AAV2/1-GFP–injected group (684.5, 516.8, and 580.7 pg/mg at the same time points, respectively), thus demonstrating the long-term expression of the recombinant protein. In the blood plasma, there was no difference in circulating FGF2 levels between AAV2/1-FGF2 and AAV2/1-GFP groups 3 mo after injection (4,664 ± 595.9 and 5,210 ± 573.5 pg/mL, respectively; $P = 0.86$). Thus, we have designed the study to be completed by 5 mo after the injection with 1×10^{10} VP per brain.

Hippocampal AAV2/1-FGF2 Injection Reverses Learning Deficit in APP+PS1 Mice. Next, to examine if AAV2/1-FGF2 injection improves spatial learning, we injected AAV2/1-FGF2 or AAV2/1-GFP control virus bilaterally into the hippocampal regions of APP+PS1 mice at two different time points (4 or 7–8 mo of age). This is based on our previous studies on APP+PS1 mice, which determined that the animals show spatial learning deficits in water maze tests at approximately 6 mo of age (28). Thus, we designed a hippocampal injection at 4 mo of age as a presymptomatic treatment, and at 7 to 8 mo of age as a postsymptomatic treatment. Injections were followed by a radial arm water maze (RAWM) task at 8 mo or 10 to 11 mo of age and neuropathological analyses at 9 mo or 11 to 12 mo of age for pre- and postsymptomatic injection studies, respectively, as described (28–30) (Fig. 1*A*). The age-matched non-Tg mouse group modeled the WT learning curve in the RAWM test as previously described (28, 30, 31) (Fig. 1 *B–D*). In contrast, among the presymptomatic treatment groups, the AAV2/1-GFP–injected APP+PS1 mice showed significantly higher errors than the non-Tg group throughout the trials (Fig. 1*B*), indicating impaired spatial memory acquisition and recall. The AAV2/1-FGF2–injected APP+PS1 mouse group showed significantly reduced error numbers at blocks 7 to 10 compared with the AAV2/1-GFP–injected APP+PS1 mice. We also examined the effect of AAV2/1-FGF2 injections as a postsymptomatic treatment (Fig. 1 *C* and *D*). Before AAV injection, both non-Tg and APP+PS1 mice were pretested by the RAWM at 7 mo of age, showing that they had already developed impaired memory formation (blocks 4–5 and 7–10, Fig. 1*C*). Three-month AAV2/1-FGF2 treatment significantly reversed the memory deficit of the APP+PS1 group to the learning curve of the non-Tg group, which was significantly lower than the APP+PS1 group with an AAV2/1-GFP injection (blocks 2–8 and 10, Fig. 1*D*). Taken together, these data indicate that chronic expression of the *FGF2* gene can protect and reverse memory acquisition and recall impairments commonly seen in the APP+PS1 mouse model of AD.

AAV2/1-FGF2 Decreases Hippocampal Aβ Deposition in APP+PS1 Mice. β-Amyloidosis is the process of Aβ aggregation from oligomer formations to diffuse plaque depositions, which eventually become compact plaques, often described and detected as thioflavin S (TS)-positive plaques. To understand the effect of chronic AAV2/1-FGF2 gene expression on β-amyloidosis, we

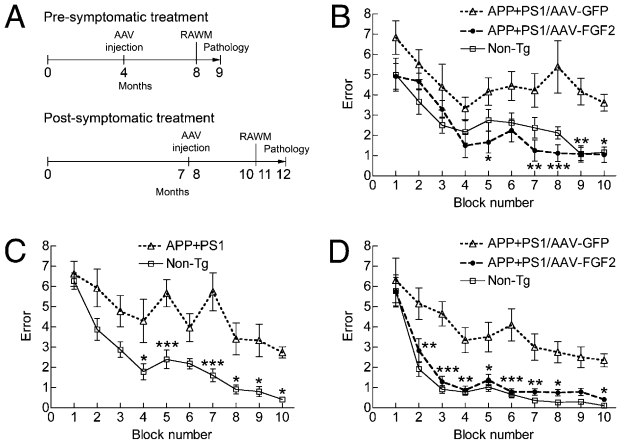

Fig. 1. Gene delivery of FGF2 improves memory function of APP+PS1 mice. (*A*) Experimental designs for pre- and postsymptomatic AAV injections into APP+PS1 mice. APP+PS1 mice received bilateral hippocampal injections of AAV2/1-GFP or AAV2/1-FGF2 at 4 mo or 7 to 8 mo of age, and were tested by a RAWM task at 8 mo or 10 to 11 mo of age ($n = 8$ per group) for pre- or postsymptomatic study, respectively. Non-Tg mice served as positive controls for the spatial learning task. (*B*) APP+PS1 mice received hippocampal injections of AAV2/1-GFP or AAV2/1-FGF2 at 4 mo of age (presymptomatic group), and were posttested in the RAWM task at 8 mo of age ($n = 8$ per group). (*C*) A preconditioning test of a RAWM task for non-Tg ($n = 12$) and untreated APP+PS1 ($n = 24$) groups was conducted at 7 mo of age. Both learning memory and recall were impaired in the APP+PS1 mice at this point. (*D*) APP+PS1 mice received hippocampal injections of AAV2/1-GFP or AAV2/1-FGF2 after the preconditioning test (postsymptomatic group), and were posttested in the RAWM task at 10 to 11 mo of age ($n = 12$ per group). $^*P < 0.05$, $^{**}P < 0.01$, or $^{***}P < 0.001$ vs. AAV2/1-GFP group (or vs. non-Tg, *C*) as determined by two-way repeated-measures ANOVA and Bonferroni posttest, respectively.

examined the area of Aβ loads in the hippocampus of AAV-injected APP+PS1 mice (Fig. 2*A*). In the presymptomatic treatment, total Aβ load (mainly diffuse plaques) and TS^+ compact plaques were partially reduced by FGF2 expression [total Aβ load, 77.1% of the GFP group ($P < 0.05$); TS^+ plaques, 67.2% of the GFP group ($P < 0.05$); Fig. 2*B*]. Although total Aβ load was not statistically different from AAV2/1-FGF2 injection in the postsymptomatic treatment (89.0% of the GFP group; $P = 0.58$), *FGF2* gene expression significantly reduced TS^+ plaque load in the hippocampal region (33.0% of the GFP group; $P < 0.05$; Fig. 2*B*). Quantification of Aβ load by ELISA in the postsymptomatic study showed that the AAV2/1-FGF2–injected group had reduced SDS-insoluble Aβ42 (fibrillar form, $P < 0.05$) but not soluble Aβ42 in the hippocampal region ($P = 0.1453$) compared with the AAV2/1-GFP–injected group (Fig. 2*C*), which was consistent with the immunohistochemistry result. On the contrary, the Aβ42 levels in the plasma showed no significant difference among groups (101.0 ± 31.7 or 93.9 ± 24.0 fmol/mg protein in the GFP or FGF2 group, respectively; $P = 0.8636$). These results demonstrate that long-term expression of the *FGF2* gene suppresses β-amyloidosis, especially the fibrillar species of Aβ aggregates, in APP+PS1 mice.

Enhanced Neurogenesis in AAV2/1-FGF2–Injected APP+PS1 Mice. As FGF2 was shown to enhance endogenous neurogenesis in the subgranular zone (SGZ) of the dentate gyrus (20, 32), we examined the effect of AAV-FGF2 on neurogenesis and differentiation by immunostaining of doublecortin (Dcx), a marker for newly generated premature neurons (Fig. 2*D*) (33). As expected, the number of Dcx^+ cells in the dentate gyrus of AAV2/1-GFP–injected APP+PS1 mice was significantly reduced (19.9% in presymptomatic treatment and 39.5% in postsymptomatic treatment

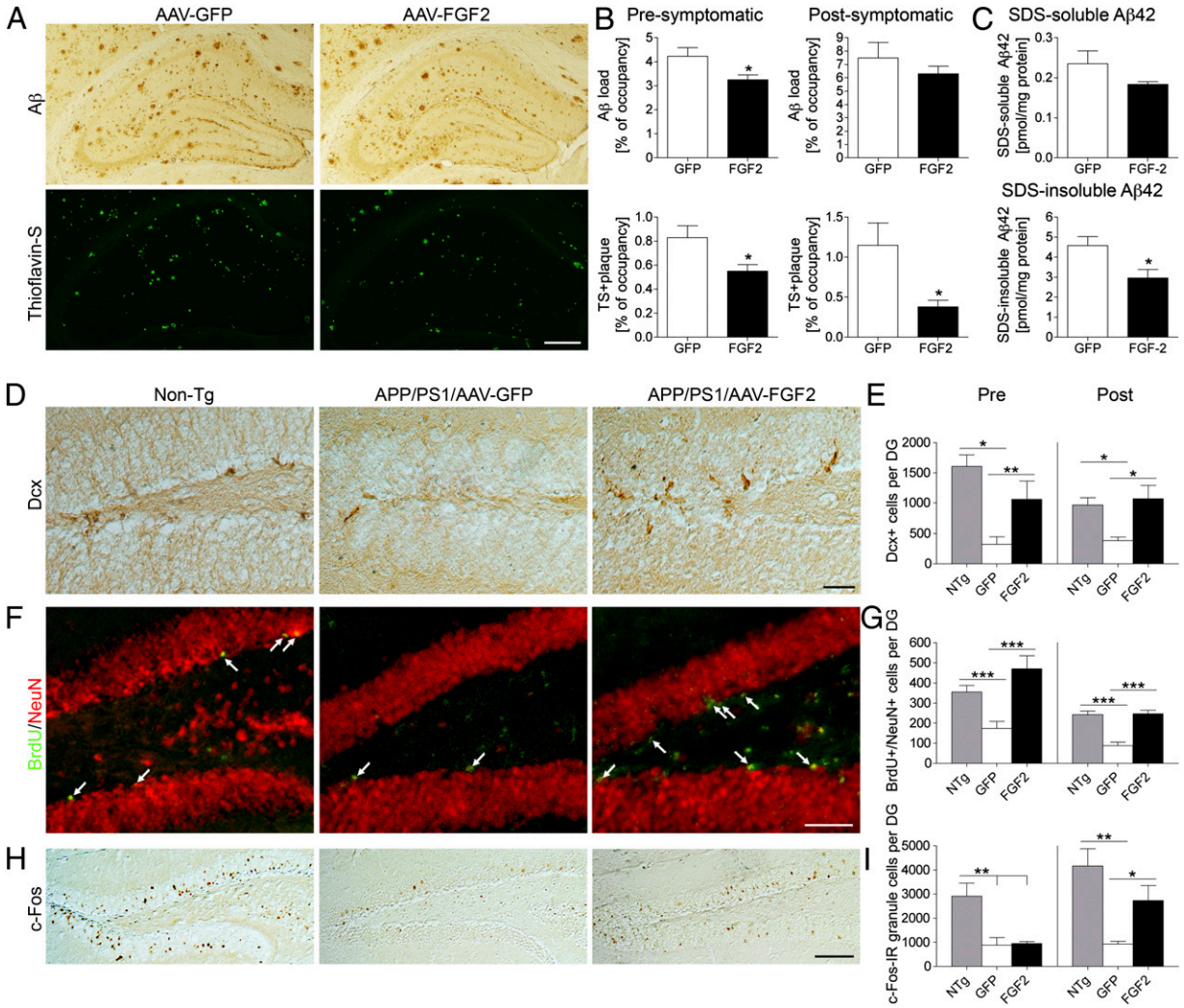

Fig. 2. Gene delivery of FGF2 reduces Aβ deposition and enhances neurogenesis in the hippocampal region of the APP+PS1 mouse brain. (*A*) Representative images of Aβ staining in the hippocampus of APP+PS1 mice in the postsymptomatic treatment. Sections were counterstained by TS for compact plaques. (Scale bar: 500 μm.) (*B*) Quantification of total Aβ load and TS$^+$ areas in hippocampal regions. Error bars represent SEM (n = 5 per group, five sections per brain). (*C*) The levels of SDS-soluble Aβ42 and SDS-insoluble Aβ42 in the brain (postsymptomatic group) were measured by human Aβ42-specific ELISA (n = 5). *$P < 0.05$ vs. AAV2/1-GFP group, as determined by Student t test. (*D*) Dcx staining in the dentate gyrus of non-Tg or APP+PS1 mice in the postsymptomatic treatment. (Scale bar: 50 μm.) (*E*) Quantification of Dcx$^+$ cells in the SGZ. (*F*) Immunofluorescence of BrdU (green) and NeuN (red) staining in the SGZ after postsymptomatic treatment. Arrows indicate BrdU$^+$/NeuN$^+$ double-positive cells. (Scale bar: 100 μm.) (*G*) Quantification of BrdU$^+$/NeuN$^+$ cells in the SGZ. Mice were intraperitoneally injected with BrdU 3 wk before the euthanasia. (*H*) c-fos staining in the dentate gyrus after the postsymptomatic treatment. (Scale bars: 200 μm.) (*I*) Quantification of c-fos$^+$ cells in the SGZ. *$P < 0.05$, **$P < 0.01$, or ***$P < 0.001$ as determined by one-way ANOVA and Newman–Keuls posttest, respectively (n = 5 per group, 10 sections per brain). Error bars represent SEM.

vs. non-Tg mice, respectively; Fig. 2*E*). Remarkably, the AAV2/1-FGF2–injected APP+PS1 mice show significantly increased numbers of Dcx$^+$ cells in the SGZ (331% increase in presymptomatic treatment or 293% increase in postsymptomatic treatment vs. AAV2/1-GFP–injected APP+PS1 mice; Fig. 2*E*), suggesting the enhancement of neuronal differentiation by FGF2 gene expression. To determine the effect of AAV2/1-FGF2 on neuronal stem cell proliferation, we have intraperitoneally injected BrdU 3 wk before euthanasia to track proliferation and maturation of BrdU incorporated cells as described (28, 29) (BrdU$^+$/NeuN$^+$ cells; Fig. 2*F*). The total BrdU$^+$ cell counts in the SGZ were increased in AAV2/1-FGF2–injected APP+PS1 mice compared with AAV2/1-GFP–injected littermates [2,329 ± 269.7 vs. 1,059 ± 34.2 in presymptomatic treatment ($P < 0.001$) and 1,789 ± 76.2 vs. 797.1 ± 55.67 in postsymptomatic treatment ($P < 0.001$)]. Similarly, the number of BrdU$^+$/NeuN$^+$ cells was significantly increased in the AAV2/1-FGF2–injected APP+PS1 mice compared with AAV2/1-GFP–injected littermates [470 ± 65.6 vs. 174 ± 34.7 in presymptomatic treatment ($P < 0.001$) and 246 ± 18.2 vs. 87.5 ± 17.0 in postsymptomatic treatment ($P < 0.001$); Fig. 2*G*]. The percentages of BrdU$^+$/NeuN$^+$ cell counts vs. total BrdU$^+$ cell counts in the dentate gyrus were 16.8%, 16.4%, and 20.1% in non-Tg, AAV2/1-GFP–injected APP+PS1 mice, and AAV2/1-FGF2–injected littermates in presymptomatic treatment, respectively, and 15.4%, 10.9%, and 13.8% in postsymptomatic treatment, respectively. These data demonstrate that neuronal stem cell proliferation and neuronal differentiation were significantly reduced in AAV2/1-GFP–injected APP+PS1 mice compared with non-Tg mice, which was significantly restored to non-Tg levels by pre- and postsymptomatic AAV2/1-FGF2 injections.

FGF2 Gene Expression Increases Neuronal c-fos Expression in the Dentate Gyrus. *c-fos* is one of the immediate-early genes induced by neural activity and behavioral training and a marker for the

activated neurons (34–37). Immediate-early gene expression plays a functional role in the neuroplastic mechanisms required for the memory consolidation processes (38, 39). To address if enhanced neurogenesis by FGF2 expression is associated with neural activation, c-fos–immunoreactive (c-fos$^+$) neurons were evaluated in the granular cell layer of the dentate gyrus in this study (Fig. 2*H*). In the presymptomatic treatment, the number of c-fos$^+$ neurons in APP+PS1 mice was reduced compared with non-Tg mice, but there was no difference between the AAV2/1-GFP and AAV2/1-FGF2 groups (Fig. 2*I*). Although the number of c-fos$^+$ neurons in the AAV2/1-GFP group was reduced compared with non-Tg mice in the postsymptomatic treatment (76.2% reduction vs. non-Tg mice), FGF2 gene expression increased the number of c-fos$^+$ neurons (297% increase vs. AAV2/1-GFP–injected APP+PS1 mice; Fig. 2*I*), suggesting that FGF2 could promote synaptic gene expression.

In Vivo Correlation of Neurogenesis and β-Amyloidosis with Spatial Learning. To determine whether β-amyloidosis and neurogenesis were correlated with cognitive function, we performed scatter-plot analyses between RAWM error counts and Aβ/TS$^+$ plaque load, Dcx$^+$, or BrdU$^+$/NeuN$^+$ cell counts for non-Tg and APP+PS1 mice with AAV2/1-GFP or AAV2/1-FGF2 injections at the pre- or postsymptomatic stages (Fig. 3). A Pearson correlation analysis indicated a significant correlation in the presymptomatic treatment of the error counts at block 10 of the RAWM test with Aβ load ($r = 0.7353$, $P = 0.0154$; Fig. 3*A*), TS$^+$ plaque load ($r = 0.7361$, $P = 0.0152$; Fig. 3*B*), Dcx$^+$ cell counts ($r = -0.6614$, $P = 0.0073$; Fig. 3*C*), or BrdU$^+$/NeuN$^+$ cells ($r = -0.7387$, $P = 0.0017$; Fig. 3*D*). Similarly, the RAWM error counts were significantly correlated with TS$^+$ plaque deposits ($r = 0.7993$, $P = 0.0055$; Fig. 3*F*), Dcx$^+$ cells ($r = -0.7074$, $P = 0.0032$; Fig. 3*G*), or BrdU$^+$/NeuN$^+$ cell counts ($r = -0.6707$, $P = 0.0062$; Fig. 3*H*), but not with total Aβ load ($r = 0.6175$, $P = 0.0571$; Fig. 3*E*) in the postsymptomatic treatment. These data clearly demonstrate that β-amyloidosis and neurogenesis are critical regulators of spatial learning in this disease mouse model.

To further understand if β-amyloidosis regulates neurogenesis in this study, we have also examined the association of the aforementioned neurogenesis-related parameters by scatter-plot analyses (Fig. S1). BrdU$^+$/NeuN$^+$ cell counts, which reflect the differentiation of the newly synthesized neurons, were negatively correlated with the total Aβ and TS$^+$ plaque loads in the presymptomatic treatment (Fig. S1 *A* and *B*). However, there was no statistical association with Dcx$^+$ cell count and β-amyloidosis in presymptomatic treatment (Fig. S1 *C* and *D*), or any of the parameters in postsymptomatic treatment (Fig. S1 *E–H*). These data indicate that mature but not premature neuronal differentiation is affected by β-amyloidosis, which is mainly diffuse plaque deposition, whereas β-amyloidosis in the later stage, which is mainly fibrillar Aβ deposition, has no consistent effect on neurogenesis.

The extent of glial inflammation was determined by the changes in the number of astrocytes and microglia accumulated around TS$^+$ plaques in the hippocampal regions of APP+PS1 mice after AAV injection (Fig. S2). The astroglial accumulation was significantly reduced in AAV2/1-FGF2–injected APP+PS1 mice compared with the AAV2/1-GFP–injected group (22% or 33% reduction after pre- or postsymptomatic treatment, respectively; $P < 0.05$; Fig. S2 *E* and *K*). However, accumulation of microglia was rather enhanced [18% or 19% ($P < 0.01$) in pre- or postsymptomatic treatment, respectively; Fig. S2 *F* and *L*]. These data demonstrate that AAV2/1-FGF2 injection enhances neurogenesis and potentially activates microglial phagocytosis of TS$^+$ plaques, leading to the reduction of Aβ deposition in the brain.

FGF2 Gene Expression Restores Long-Term Potentiation Deficits in J20 Mice. Synaptic plasticity and long-term potentiation (LTP) underlie the experience-dependent modification of behavior (40). To explore possible alterations in synaptic transmission and plasticity in areas of the brain most associated with learning and memory, we studied LTP in the Schaffer-collateral pathway to CA1 synapses in hippocampal slices. In this study, a platelet-derived growth factor promoter-driven APP mutant Tg mouse model of AD (PDAPP mouse line J20) was used because this mouse model has demonstrated a significant deficit in LTP as it ages (41). Through the induction of LTP in the CA1 region of the hippocampus, the differences between LTP induced by high-fre-

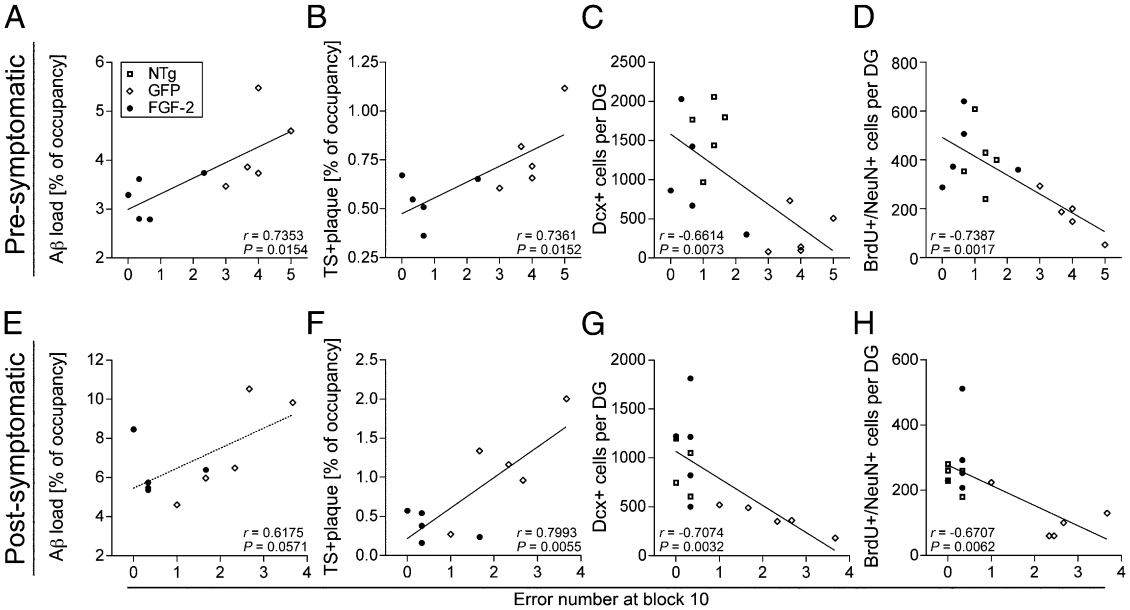

Fig. 3. Significant correlations between spatial learning and β-amyloidosis or neurogenesis. Pearson correlation analysis shows a significant correlation (*r* value) between the error number at block 10 of the RAWM test and total Aβ load (*A*, but not *E*), TS$^+$ plaque load (*B* and *F*), Dcx$^+$ cell count (*C* and *G*), and BrdU$^+$/NeuN$^+$ cell count (*D* and *H*) in presymptomatic (*A–D*) and postsymptomatic treatments (*E–H*).

quency stimulation (HFS; 100 Hz) among the three groups were compared. A robust LTP was recorded in non-Tg mice, with an average magnitude of 192.0 ± 9.1% of basal level when measured 45 min after HFS (n = 13; Fig. 4 *A*–*C*). In contrast, the LTP magnitude recorded in hippocampal slices from the AAV2/1-GFP group was 137.3 ± 8.4% of basal level, which is a significant deficit compared with the non-Tg mouse group (n = 10; $P < 0.01$; Fig. 4 *B* and *C*). However, pretreatment of the Tg mice with AAV2/1-FGF2 exhibited protective effects on synaptic plasticity, with an average LTP magnitude of 163.5 ± 9.2% of basal level (n = 9), suggesting that FGF2 gene expression enhances synaptic transmission and plasticity in CA1 synapses of the hippocampus. In addition, AAV2/1-FGF2 treatment significantly increased short-term potentiation (STP) but not posttetanic potentiation (PTP) compared with the AAV2/1-GFP–injected group, which showed significant reduction of STP and PTP compared with the non-Tg group (Fig. 4*C*). These data demonstrate that FGF2 treatment can enhance STP and LTP but not PTP in the CA1 region.

FGF2 Enhances Aβ Phagoyctosis in Primary Cultured Microglia and Aβ Production in Primary Cultured Neurons. To elucidate how FGF2 gene expression enhances Aβ clearance in the APP+PS1 mouse brain, we have cultured mouse primary microglia and tested the effect of FGF2 on Aβ uptake in vitro (Fig. 5 *A*–*M*). Microglia were treated with different doses of FGF2 for 24 h, followed by incubation with fibrillar Aβ42 for 30 min. Aβ uptake was quantified as immunofluorescence intensity and normalized by nuclear staining as previously described (42). FGF2 enhances Aβ phagocytosis in a dose-dependent manner, demonstrating the direct effect of FGF2 on Aβ clearance. In addition, we have also examined the effect of AAV2/1-FGF2 infection on Aβ production in vitro. Primary neurons were infected with AAV2/1-FGF2 or AAV2/1-GFP as a control. Three days after the infection, secreted and cytoplasmic FGF2 was detected in AAV2/1-FGF2 infected but not AAV2/1-GFP-infected or uninfected neurons (Fig. 5 *N* and *O*). Endogenous FGF2 was only detected in the nuclear fraction, and approximately 99% of expressed FGF2 was detected in the intracellular fraction, suggesting the intracellular function of FGF2 in neurons. As different FGF2 isoforms (18 kDa as a low molecular weight and secreted isoform, and 22 and 24 kDa as high molecular weight and intracellular isoforms), the subcellular distribution of recombinant FGF2 isoforms was determined in AAV-infected neurons. FGF2 protein was mostly localized in the nuclear-enriched fraction as 18-, 22-, and 24-kDa isoforms (Fig. 5 *O* and *P*). In the cytoplasm-enriched fraction, only the 18-kDa isoform was detected. Finally, mouse primary cultured neurons were infected with adenovirus expressing Swedish familial AD APP_{695} mutant, followed by infection with AAV2/1-FGF2. Production of Aβ42 was significantly inhibited by AAV2/1-FGF2 infection compared with AAV2/1-GFP or uninfected neurons (Fig. 5*Q*). These results suggest that the expression of high molecular weight FGF2 in neurons inhibits Aβ42 production.

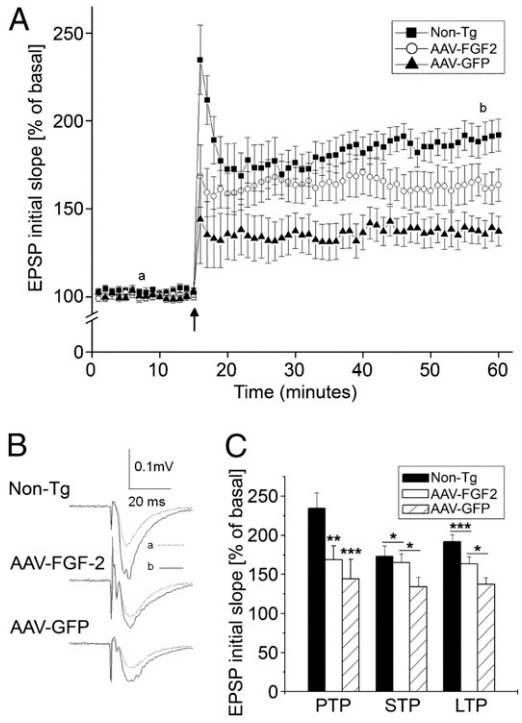

Fig. 4. Chronic expression of FGF2 attenuates the deficit in LTP in PDAPP (J20) mice. (*A*) The time course and average magnitude of LTP recorded in the CA1 dendritic field (stratum radium) of hippocampal slices prepared from 5-mo-old J20 mice injected with AAV2/1-GFP (10 slices from four mice), AAV2/1-FGF2 (nine slices from four mice) and non-Tg controls (13 slices from five mice). The graph plots the initial slope of the field EPSPs evoked in response to constant current stimulation. HFS (100 Hz) was delivered at the time indicated by an arrow. Each point in this graph represents an average of three consecutive sweeps. (*B*) Representative field EPSPs taken 7 min before (dotted line) and 43 min after (solid line) HFS in different experimental groups as indicated. (*C*) A summary bar graph showing the magnitudes of PTP, STP, and LTP recorded from mice injected with AAV2/1-GFP, AAV2/1-FGF2, or non-Tg controls. $*P < 0.05$, $**P < 0.01$, or $***P < 0.001$ as determined by one-way ANOVA and Tukey post-hoc test, respectively. Error bars represent SEM.

AAV-FGF2 Enhances Neurogenesis of Neural Stem Cells. Finally, to directly evaluate the effect of AAV2/1-FGF2 and Aβ on neural stem cell differentiation, we have infected mouse neural stem cells in proliferation condition with AAV2/1-GFP or AAV2/1-FGF2, and differentiated them in the presence or absence of 1 μM Aβ42 oligomer (Fig. 6 *A* and *B*). The purity of the neural stem cells was confirmed by immunostaining with specific markers (nestin, a neural stem cell marker, and Ki67, a proliferating cell marker; Fig. S3). As the neural stem cells were yet to be differentiated into neural progenitor cells in this condition, dissociated neural stem cells were mainly differentiated to astrocytes or remained in the undifferentiated state (Fig. 6 *A* and *B*). AAV2/1-FGF2 infection significantly enhances neuronal differentiation compared with AAV2/1-GFP–injected cells (26.9 ± 7.0% vs. 12.2 ± 5.5%; $P < 0.01$; Fig. 6 *A* and *B*) as well as astrocytic differentiation (70.0 ± 6.5% vs. 47.6 ± 4.1%; $P < 0.05$), and Aβ oligomer treatment potently diminished neuronal differentiation (26.9 ± 7.0% vs. 1.1 ± 1.1%; $P < 0.001$; Fig. 6 *A* and *B*). On the contrary, treatment of neural stem cells with a low dose of FGF2 (2 ng/mL) or Aβ42 oligomer reduced the astrocytic differentiation of neural stem cells (61.7 ± 4.5% in the PBS solution group vs. 40.2 ± 6.0% in the FGF2 group or 39.4 ± 4.4% in the Aβ42 oligomer group; $P < 0.05$ or $P < 0.01$, respectively; Fig. 6 *C* and *D*). Cotreatment with Aβ42 oligomer and FGF2 had no effect on neuronal differentiation among the four groups in this experimental design. These data indicate that AAV2/1-FGF2 infection has a unique effect on neural stem cell differentiation, which is distinct from the effect of extracellular treatment of FGF2.

Discussion

Our study clearly shows that bilateral hippocampal injection of AAV2/1-FGF2 in APP+PS1 mice enhanced spatial learning, neurogenesis in the SGZ, and partial amyloid clearance in pre- and postsymptomatic treatments. Enhanced Aβ clearance is associated with significant accumulation of microglia and reduced astrogliosis around TS^+ compact plaques, suggesting the Aβ phagocytosis-induced anti-inflammatory response of microglia

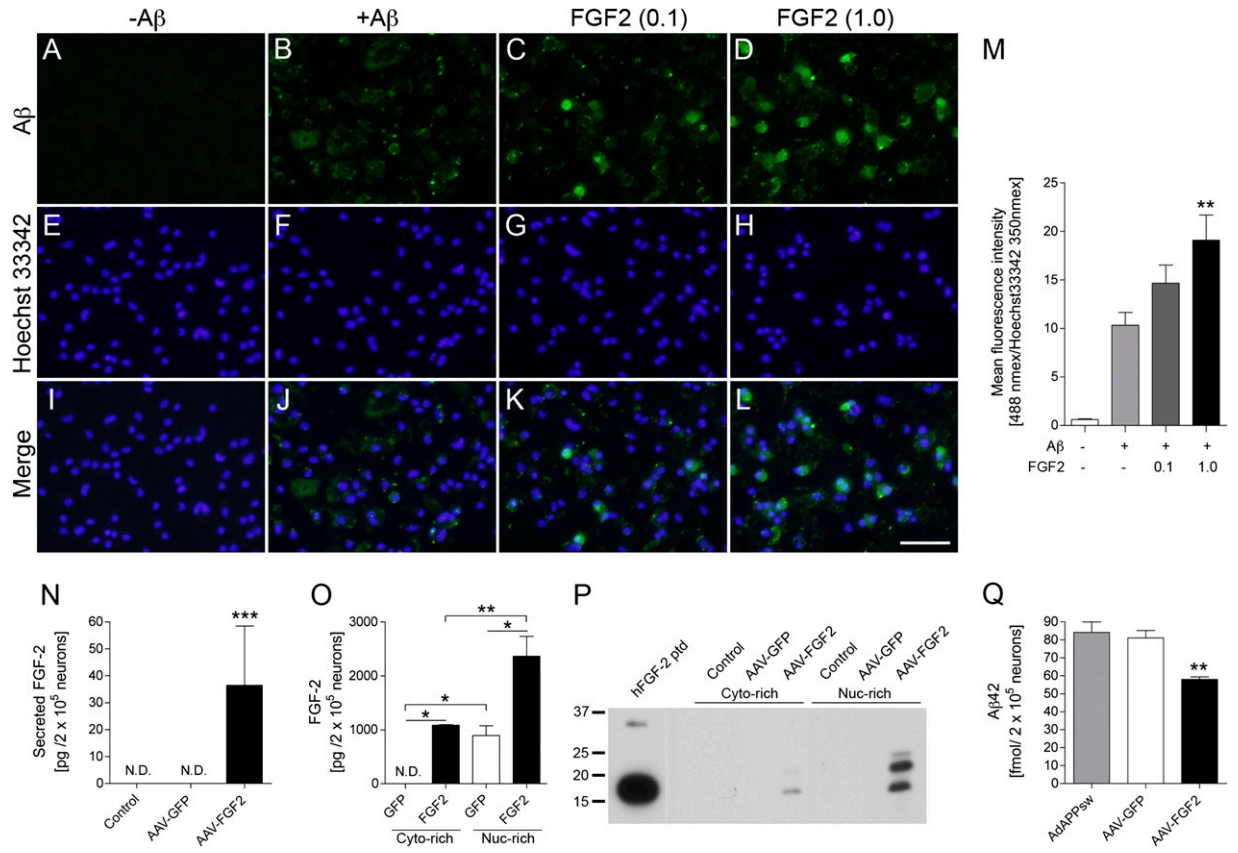

Fig. 5. FGF2 enhances Aβ phagocytosis in primary microglia and inhibits Aβ production from primary neurons. (*A–M*) Primary mouse microglia were incubated with or without fibrillar Aβ42 (±Aβ) and recombinant murine FGF2 protein (0.1 or 1.0 ng/mL) for 1 h, followed by immunofluorescence for Aβ (green; *A–D*) and cell nuclei (blue; *E–H*). Merged captured images are also shown (*I–L*). (Scale bar: 50 μm.) (*M*) Quantification of Aβ fluorescence intensity (excitation/emission wavelengths, 488 nm/519 nm) normalized by Hoechst 33342 intensity (excitation/emission wavelengths, 350 nm/461 nm). $^{**}P < 0.01$ vs. +Aβ group as determined by one-way ANOVA and Newman–Keuls posttest, respectively ($n = 6$ per group). Error bars represent SEM. (*N–Q*) Mouse primary cultured neurons (200,000 cells per well in 48-well plate) were infected with or without AAV2/1-GFP (4×10^{10} VP per 500 μL medium), or AAV2/1-FGF2 (4×10^{10} VP per 500 μL medium) for 3 d. (*N*) FGF2 secretion from the neurons (undetectable from uninfected or AAV2/1-GFP–infected cells; 36.50 ± 22.02 pg per 200,000 neurons from AAV2/1-FGF2–infected cells). (*O* and *P*) AAV2/1-infected neurons were fractionated into cytoplasm (Cyto)-rich and nuclear (Nuc)-rich fractions, and subjected to FGF2 ELISA (*N*) or immunoblotting (*P*). hFGF2 ptd; 18-kDa human FGF2 recombinant peptide. (*Q*) Mouse primary cultured neurons (200,000 cells per well in a 48-well plate) were infected with adenovirus expressing Swedish familial AD APP_{695} mutant (AdAPPsw) for 1 h. After washing and one-overnight incubation, the neurons were infected with or without AAV2/1-GFP or AAV2/1-FGF2 for 3 d. Tissue culture media was subjected to Aβ42 ELISA. $^{*}P < 0.05$, $^{**}P < 0.01$, or $^{***}P < 0.001$ as determined by one-way ANOVA and Newman–Keuls posttest, respectively ($n = 3$ per group). Error bars represent SEM.

suppressed the astrogliosis in the close proximity. Enhanced neuronal activity is also demonstrated in the increased number of c-fos$^+$ cell counts in the dentate gyrus of APP+PS1 mice and restored CA1 LTP in J20 mice after AAV2/1-FGF2 injection. In vitro studies demonstrate that FGF2 treatment of primary cultured microglia enhances Aβ phagocytosis, and AAV2/1-FGF2 infection of primary cultured neurons reduces Aβ production. AAV2/1-FGF2 transduction but not FGF2 treatment enhances neuronal differentiation of neural stem cells, and this effect is sensitive to Aβ oligomer cotreatment.

AAV2/1-FGF2 Treatment on Spatial Learning and Neurogenesis. The age-associated spatial learning deficit was well documented in several animal models of AD, including APP+PS1 mice (7, 28, 30, 43). The significant restoration of spatial learning in AAV2/1-FGF2–injected APP+PS1 mice after pre- and postsymptomatic treatments suggests that FGF2 gene therapy is effective in potentially ameliorating cognitive dysfunction after the onset of symptoms. This is an advancement in AAV-mediated gene therapy vs. our previous studies in which injection of AAV expressing CCL2 dominant-negative mutant, IL-4, or IL-10 were all ineffective at the postsymptomatic stage (28, 30). This is also in line with the report that anti-inflammatory therapy could be effective only as prophylactic therapy, as determined by the clinical trials of nonsteroidal anti-inflammatory drugs (naproxen and celecoxib) on patients with AD (44); therefore, this FGF2 study provides a potential postsymptomatic intervention that could not be achieved by anti-inflammatory treatment alone.

Accumulating evidence suggests that neurocognitive impairments are parallel to neurogenic deficits (45–47). Neurogenic impairment is evident in the APP+PS1 mice at both 9 and 12 mo of age, which is consistent with other AD mouse models that overexpress mutated human APP or PS1 (48–51). AAV2/1-FGF2 injection significantly enhances the neurogenesis in two different maturation stages (Dcx$^+$ and BrdU$^+$/NeuN$^+$ cells). The enhancement of the number of BrdU$^+$/NeuN$^+$ mature neurons by FGF2 gene expression is particularly important for its clinical application, as the earlier study showed enhanced neuronal division but impaired maturation in the AD brain (52). Indeed, our scatter-plot study clearly demonstrates that the numbers of Dcx$^+$ and BrdU$^+$/NeuN$^+$ cell counts are closely associated with improved spatial learning. In accord, treatment of another AD Tg mouse model (3xTg-AD mouse) with allopregnanolone shows a close positive correlation of enhanced

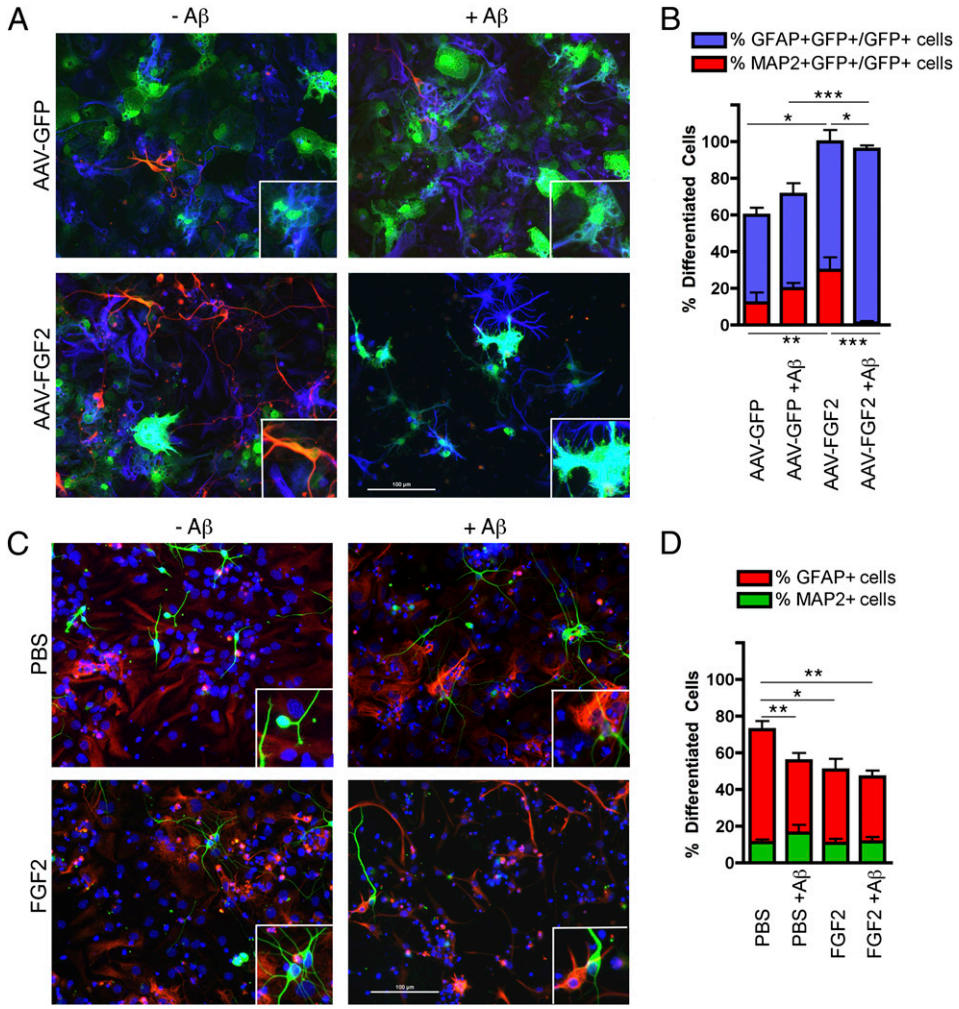

Fig. 6. AAV2/1-FGF2 enhances differentiation of mouse neural stem cells. (*A*) Dissociated mouse neuronal stem cells infected with AAV2/1-GFP (1.5×10^{10} VP) or AAV2/1-FGF2 + AAV2/1-GFP (1.5×10^{10} plus 1.5×10^{9} VP) were incubated with or without 1 μM Aβ42 oligomer for 7 d, followed by immunofluorescence for MAP-2 (neuronal marker; red), GFAP (astrocytic marker; blue), and GFP (all AAV-infected cells; green). (*B*) Quantification of percentage of MAP-2$^+$/GFP$^+$ and GFAP$^+$/GFP$^+$ cells over the total number of GFP$^+$ cells (n = 10 fields of view per group). (*C*) Uninfected dissociated mouse neuronal stem cells were incubated with or without 1 μM Aβ42 oligomer, in the presence or absence of FGF2 (2 ng/mL) for 7 d, followed by immunofluorescence of MAP-2 (green), GFAP (red), and Hoechst 33342 (blue). (*D*) Quantification of percentage of MAP-2$^+$ and GFAP$^+$ cells over the total number of Hoechst 33342-expressing cells (n = 10 fields of view per group). (*A* and *C*) Original magnification of 200×; inset, 2× magnification of the field. (*B* and *D*) Columns represent mean ± SEM; $P < 0.05$, $^{**}P < 0.01$, or $^{***}P < 0.001$ between two groups as determined by ANOVA and Tukey post-hoc test.

neurogenesis (BrdU$^+$ cell count) in the SGZ and improved memory performance (53). Taken together, these studies strongly support the therapeutic potential of the enhancement of neurogenesis at the SGZ of the dentate gyrus in AD brains.

AAV-FGF2 Treatment on β-Amyloidosis and Its Effect on Neurogenesis. Total Aβ and TS$^+$ plaque loads are negatively associated with spatial learning in presymptomatic treatment, and only TS$^+$ plaque load is associated in postsymptomatic treatment. Thus, β-amyloidosis is a critical regulator for spatial learning in the APP+PS1 mouse brain. AAV2/1-FGF2–injected APP+PS1 mice show modest reduction in total Aβ and TS$^+$ plaque load accompanied by enhanced microgliosis around the plaque regions, suggesting that microglia may play an important role in Aβ clearance in this study. This is confirmed in the in vitro study that FGF2 directly activates the Aβ phagocytosis by primary cultured microglia in a dose-responsive manner. As far as we are aware, there has previously been no report about the effect of FGF2 on microglial phagocytosis of Aβ. Aβ phagocytosis may also induce an anti-inflammatory response in microglia (54), which potentially leads to the reduced astrogliosis around the plaque region. Furthermore, we also show the reduction in Aβ production from AAV2/1-FGF2–infected neurons. These results demonstrate that there is a potential cellular mechanism of reduced β-amyloidosis that is induced by AAV-FGF2 injection; however, this exact mechanism has yet to be determined.

The effect of Aβ on neurogenesis has been a matter of debate; differences in Aβ lengths and aggregation (e.g., Aβ40 and Aβ42 in monomeric, oligomeric, or fibrillar forms) and stem cell sources (e.g., preparation from mouse, rat, human embryonic, or adult brain) in different tissue culture conditions have resulted in different outcomes (for a recent review, see ref. 55). One of the relatively consistent observations is that Aβ oligomers have been shown to enhance neural stem cell proliferation, whereas neuronal differentiation can be inhibited by the neurotoxic or astrogliogenic effects of Aβ in different forms (55). We show that the number of BrdU$^+$/NeuN$^+$ but not Dcx$^+$ cell counts is negatively correlated with the number of diffuse or compact plaques in the presymptomatic injection study. As NeuN$^+$ cells are at a more mature stage than Dcx$^+$ cells, this suggests that neuronal

maturation was affected by the local Aβ deposition. This is in line with the result of our in vitro study of AAV-FGF2–infected neural stem cells, in which Aβ oligomers inhibit the neuronal differentiation. The sensitivity to Aβ on AAV2/1-FGF2–induced neurogenesis suggests that the local Aβ clearance is beneficial for the maturation of neuronal cells in the SGZ as demonstrated in the presymptomatic treatment.

Mechanism of AAV2/1-FGF2–Induced Neurogenesis and Neuronal Activation. FGF2 concentration regulates the rate of cell proliferation and generation of neuronal/glial differentiation: lower concentrations induce neurogenesis, whereas higher concentrations induce astrogliogenesis (26, 56). Our study shows that AAV2/1-FGF2 infection directly enhances neuronal differentiation of neural stem cells in vitro, which is apparently a different mode of action from the effect of soluble FGF2 (18 kDa) in the same experimental condition. This could be explained by the gene expression of high molecular weight FGF2 isoforms (22 and 24 kDa) and their distinct nuclear localization after AAV2/1-FGF2 transduction. Interestingly, FGFR1 acts as a nuclear protein (57) and mediates integrative nuclear FGFR1 signaling (58), which is specific to its ligation with high molecular weight isoforms but not with the 18-kDa FGF2 (59). This pathway activates transcriptional coactivator CREB-binding protein, thereby up-regulating gene activities associated with differentiation and development of neuronal cells (60). Thus, it is possible that intracellular high molecular weight FGF2 enhances neuronal differentiation through the nuclear FGFR1 signaling pathway. Additionally, this pathway is potentially important for the AAV-FGF2–induced enhancement of hippocampal synaptic activity as demonstrated by the significant recovery of CA1 LTP in J20 mice and c-fos expression in the dentate gyrus of AAV-FGF2–injected APP+PS1 mice.

These results prompted us to develop a hypothesis that unifies the biological interaction of FGF2, Aβ, and hippocampal functions (*Author Summary*, Fig. P1). The proliferation of self-renewing neuronal stem cells in the SGZ is enhanced by endogenous FGF2 mainly secreted from astrocytes and potentially by direct stimulation with Aβ (55). AAV2/1-FGF2 infection of the neuronal stem cells expresses intracellular FGF2 gene expression and enhances neuronal differentiation via a distinct mechanism from the secreted FGF2. Neuronal maturation is enhanced by the FGF2 gene expression in the neuronal stem cells and is inhibited by Aβ. Neurons also produce Aβ, which is partially inhibited by FGF2 gene expression. FGF2 gene expression in neurons enhances c-fos expression and hippocampal LTP, and confers the synaptic inhibition by Aβ. Enhanced neuronal plasticity may lead to hippocampal learning. FGF2 also activates microglial recruitment and enhances its Aβ uptake, leading to the partial reduction of Aβ plaques in the brain.

In conclusion, we have demonstrated that AAV-mediated gene expression of FGF2 in APP+PS1 mice significantly restores spatial learning, neurogenesis, and partial Aβ clearance in the hippocampal regions after pre- and postsymptomatic treatment. AAV-FGF2 injection also enhances CA1 LTP in J20 mice. Further investigation is warranted to understand the molecular mechanism of AAV2/1-FGF2–induced enhancement in neurogenesis and neurocognitive function for its therapeutic applications to AD and other neurocognitive disorders.

Materials and Methods

Animals. APP+PS1 and non-Tg littermates were generated by crossing Tg2576 mice expressing the Swedish mutation of human APP_{695} with PS1 mutant mice (M146L line 6.1) in B6/129 strain (43, 61). Genotyping was performed by genomic PCR as described previously to identify APP transgene-positive mice (43). All animal use procedures were strictly reviewed by the institutional animal care and use committees of University of Nebraska Medical Center and Boston University School of Medicine.

AAV2/1-FGF2 Virus Preparation and Stereotaxic Injection. For pAAV2-FGF2 *cis* plasmid construction, human FGF2 cDNA (IMAGE clone 1690025) was sublconed into AAV2 *cis* vector (pAAV2-MCS-WPRE) (28, 30, 62). AAV2/1 hybrid virus expressing FGF2 or GFP was prepared as described (28, 30, 63, 64). AAV2/1 viruses (2 μL of saline solution containing AAV2/1-GFP or AAV2/1-FGF2, 1×10^{10} VP per brain) were stereotaxically injected into mouse hippocampus bilaterally as described (28–30).

Immunohistochemistry. Immunohistochemistry was performed by using specific antibodies to identify pan-Aβ (rabbit polyclonal, 1:100; Zymed), c-fos (rabbit polyclonal, 1:10,000; Calbiochem), Dcx (goat polyclonal, 1:500; Santa Cruz Biotechnology), anti-BrdU (6 μg/mL, mouse monoclonal; Roche Diagnostics), and biotin-conjugated anti-NeuN (mouse monoclonal, 1:500; Millipore) as described (28–30, 42). For quantification analysis, the areas of Aβ loads and TS^+ plaques, and the numbers of Dcx and $BrdU^+$/$NeuN^+$ cells per dentate gyrus, were quantified as described (29, 30, 65, 66).

ELISA and Western Blotting. Protein extraction and Aβ ELISA (Aβ40 and Aβ42) was performed as described (4). FGF2 was measured by using commercially available enzyme immunoassays (human FGF-basic ELISA Development Kit; Peprotech). Immunoblotting was performed by using anti-FGF2 pAb (Peprotech) according to the manufacturer's instructions.

Hippocampal Electrophysiology. Mouse CA1 hippocampal electrophysiology was performed as previously described (67, 68). The initial slope of the field excitatory postsynaptic potential (fEPSP) was analyzed and expressed as percentage of basal level (the average of initial slopes from the first 30 min was treated as 100%, i.e., the basal level). In bar graphs, the magnitudes of PTP, STP, and LTP were quantified at the time point of 50 min after HFS.

Primary Tissue Culture Studies. Mouse primary cortical neurons were prepared as described previously (69), and infected with AAV2/1-GFP or AAV2/1-FGF2 (4×10^{10} VP per 200,000 cells in 500 μL). For a measurement of Aβ production, neurons were infected with recombinant adenovirus-expressing Swedish APP mutation 1 d before infection with AAV as described previously (66). Three days after infection with AAV, the neurobasal medium, a cytoplasm-enriched fraction, and a nuclear-enriched fraction were subjected to Aβ ELISA and FGF2 immunoblotting.

Mouse primary microglia (5×10^4 cells per well in a 96-well plate) were cultured from postnatal day 0 pups as described previously (42). After preincubation of microglia with recombinant mouse FGF2 (0.1 or 1.0 ng/mL; R&D Systems), microglia were incubated with or without 10 μM fibrillar Aβ42 (Invitrogen) for 1 h, then fixed with freshly depolymerized 4% paraformaldehyde for immunofluorescence-based microplate reading system as described (42, 70).

Primary neural stem cell cultures were prepared from mouse embryonic brain at embryonic day 14 as previously described (29, 71). Briefly, cells were cultured as neurospheres for 7 d until spheres reached 100 to 150 μm in diameter. Neurospheres were collected and mechanically dissociated by trituration in complete proliferation media with or without AAV2/1-GFP (1.5×10^{10} VP per 500 μL) or AAV2/1-FGF2 plus AAV2/1-GFP (1.5×10^{10} plus 0.15×10^{10} VP per 500 μL, respectively), and then plated onto poly-D-lysine and laminin (both from Sigma-Aldrich)–coated coverslips (18 mm in diameter) in 24-well cell culture plates at a density of 125,000 cells per well. The media was changed to fresh differentiation media (Neurobasal media, B27, and 1× penicillin/streptomycin; Invitrogen) in the presence or absence of Aβ42 oligomer (1 μM) or recombinant FGF2 (2 ng/mL, for AAV uninfected groups). Aβ42 oligomer was prepared from synthetic Aβ42 as previously described (72). After a total of 7 d in culture, the cells were fixed in 4% paraformaldehyde in PBS solution and subjected to immunofluorescence for GFAP, microtubule-associated protein–2 (MAP-2), and DAPI, and the captured images were quantified as described (29).

Statistics. All data were normally distributed and are presented as mean values ± SEM. In the case of single mean comparison, data were analyzed by Student *t* test. In case of multiple mean comparisons, the data were analyzed by ANOVA and Newman–Keuls posttest, or two-way repeated-measures ANOVA, followed by Bonferroni multiple comparison tests using statistics software (Prism 4.0; GraphPad). *P* values less than 0.05 were regarded to reflect a significant difference.

ACKNOWLEDGMENTS. We thank Drs. K. Hsiao-Ashe for providing the Tg2576 mice, K. Duff for providing the M146L PS1 mice, and R. Klein for pGFP plasmid, the University of Pennsylvania Gene Therapy Program for the

recombinant AAV1 vectors, R. Swan for assistance in immunohistochemistry, J. Keblesh for assistance in electrophysiology, and S. Ikezu for manuscript editing. This work was supported in part by the Vada Kinman Oldfield Alzheimer's Research Fund (T.K. and T.I.), the Boston University Start-up Fund (T.I.), and National Institutes of Health Grants NS043985 and AG032600 (to T.I.).

1. Martin JB (1999) Molecular basis of the neurodegenerative disorders. *N Engl J Med* 340:1970–1980.
2. Forman MS, Trojanowski JQ, Lee VM (2004) Neurodegenerative diseases: A decade of discoveries paves the way for therapeutic breakthroughs. *Nat Med* 10:1055–1063.
3. Selkoe DJ (2002) Alzheimer's disease is a synaptic failure. *Science* 298:789–791.
4. Mattson MP (2004) Pathways towards and away from Alzheimer's disease. *Nature* 430:631–639.
5. Blennow K, de Leon MJ, Zetterberg H (2006) Alzheimer's disease. *Lancet* 368:387–403.
6. Schenk D, et al. (1999) Immunization with amyloid-beta attenuates Alzheimer-disease-like pathology in the PDAPP mouse. *Nature* 400:173–177.
7. Morgan D, et al. (2000) A beta peptide vaccination prevents memory loss in an animal model of Alzheimer's disease. *Nature* 408:982–985.
8. Bard F, et al. (2003) Epitope and isotype specificities of antibodies to beta -amyloid peptide for protection against Alzheimer's disease-like neuropathology. *Proc Natl Acad Sci USA* 100:2023–2028.
9. Hock C, et al. (2003) Antibodies against beta-amyloid slow cognitive decline in Alzheimer's disease. *Neuron* 38:547–554.
10. Birmingham K, Frantz S (2002) Set back to Alzheimer vaccine studies. *Nat Med* 8:199–200.
11. Check E (2002) Nerve inflammation halts trial for Alzheimer's drug. *Nature* 415:462.
12. Carlson C, et al. (2011) Prevalence of asymptomatic vasogenic edema in pretreatment Alzheimer's disease study cohorts from phase 3 trials of semagacestat and solanezumab. *Alzheimers Dement* 7:396–401.
13. Imbimbo BP, Giardina GA (2011) γ-secretase inhibitors and modulators for the treatment of Alzheimer's disease: Disappointments and hopes. *Curr Top Med Chem* 11:1555–1570.
14. Tuszynski MH, et al. (2005) A phase 1 clinical trial of nerve growth factor gene therapy for Alzheimer disease. *Nat Med* 11:551–555.
15. Nagahara AH, et al. (2009) Neuroprotective effects of brain-derived neurotrophic factor in rodent and primate models of Alzheimer's disease. *Nat Med* 15:331–337.
16. Bishop KM, et al. (2008) Therapeutic potential of CERE-110 (AAV2-NGF): Targeted, stable, and sustained NGF delivery and trophic activity on rodent basal forebrain cholinergic neurons. *Exp Neurol* 211:574–584.
17. Wu K, et al. (2005) AAV2/5-mediated NGF gene delivery protects septal cholinergic neurons following axotomy. *Brain Res* 1061:107–113.
18. Mudò G, et al. (2009) The FGF-2/FGFRs neurotrophic system promotes neurogenesis in the adult brain. *J Neural Transm* 116:995–1005.
19. Jin K, et al. (2003) Neurogenesis and aging: FGF-2 and HB-EGF restore neurogenesis in hippocampus and subventricular zone of aged mice. *Aging Cell* 2:175–183.
20. Kuhn HG, Winkler J, Kempermann G, Thal LJ, Gage FH (1997) Epidermal growth factor and fibroblast growth factor-2 have different effects on neural progenitors in the adult rat brain. *J Neurosci* 17:5820–5829.
21. Tao Y, Black IB, DiCicco-Bloom E (1997) In vivo neurogenesis is inhibited by neutralizing antibodies to basic fibroblast growth factor. *J Neurobiol* 33:289–296.
22. Baldauf K, Reymann KG (2005) Influence of EGF/bFGF treatment on proliferation, early neurogenesis and infarct volume after transient focal ischemia. *Brain Res* 1056:158–167.
23. Sapieha PS, Peltier M, Rendahl KG, Manning WC, Di Polo A (2003) Fibroblast growth factor-2 gene delivery stimulates axon growth by adult retinal ganglion cells after acute optic nerve injury. *Mol Cell Neurosci* 24:656–672.
24. Schuettauf F, et al. (2004) Adeno-associated viruses containing bFGF or BDNF are neuroprotective against excitotoxicity. *Curr Eye Res* 29:379–386.
25. Chen K, Henry RA, Hughes SM, Connor B (2007) Creating a neurogenic environment: The role of BDNF and FGF2. *Mol Cell Neurosci* 36:108–120.
26. Chen H, Tung YC, Li B, Iqbal K, Grundke-Iqbal I (2007) Trophic factors counteract elevated FGF-2-induced inhibition of adult neurogenesis. *Neurobiol Aging* 28: 1148–1162.
27. Cummings BJ, Su JH, Cotman CW (1993) Neuritic involvement within bFGF immunopositive plaques of Alzheimer's disease. *Exp Neurol* 124:315–325.
28. Kiyota T, et al. (2010) CNS expression of anti-inflammatory cytokine interleukin-4 attenuates Alzheimer's disease-like pathogenesis in APP+PS1 bigenic mice. *FASEB J* 24:3093–3102.
29. Kiyota T, et al. (2011) AAV serotype 2/1-mediated gene delivery of anti-inflammatory interleukin-10 enhances neurogenesis and cognitive function in APP+PS1 mice. *Gene Ther*, 10.1038/gt.2011.126.
30. Kiyota T, et al. (2009) AAV1/2-mediated CNS gene delivery of dominant-negative CCL2 mutant suppresses gliosis, beta-amyloidosis, and learning impairment of APP/PS1 mice. *Mol Ther* 17:803–809.
31. Wilcock DM, et al. (2004) Passive immunotherapy against Abeta in aged APP-transgenic mice reverses cognitive deficits and depletes parenchymal amyloid deposits in spite of increased vascular amyloid and microhemorrhage. *J Neuroinflammation* 1:24.
32. Wagner JP, Black IB, DiCicco-Bloom E (1999) Stimulation of neonatal and adult brain neurogenesis by subcutaneous injection of basic fibroblast growth factor. *J Neurosci* 19:6006–6016.
33. Rao MS, Shetty AK (2004) Efficacy of doublecortin as a marker to analyse the absolute number and dendritic growth of newly generated neurons in the adult dentate gyrus. *Eur J Neurosci* 19:234–246.
34. Abraham WC, et al. (1993) Correlations between immediate early gene induction and the persistence of long-term potentiation. *Neuroscience* 56:717–727.
35. Worley PF, et al. (1993) Thresholds for synaptic activation of transcription factors in hippocampus: correlation with long-term enhancement. *J Neurosci* 13:4776–4786.
36. Seeds NW, Williams BL, Bickford PC (1995) Tissue plasminogen activator induction in Purkinje neurons after cerebellar motor learning. *Science* 270:1992–1994.
37. Vann SD, Brown MW, Aggleton JP (2000) Fos expression in the rostral thalamic nuclei and associated cortical regions in response to different spatial memory tests. *Neuroscience* 101:983–991.
38. Robertson HA (1992) Immediate-early genes, neuronal plasticity, and memory. *Biochem Cell Biol* 70:729–737.
39. Dragunow M (1996) A role for immediate-early transcription factors in learning and memory. *Behav Genet* 26:293–299.
40. Malenka RC, Bear MF (2004) LTP and LTD: An embarrassment of riches. *Neuron* 44:5–21.
41. Saganich MJ, et al. (2006) Deficits in synaptic transmission and learning in amyloid precursor protein (APP) transgenic mice require C-terminal cleavage of APP. *J Neurosci* 26:13428–13436.
42. Kiyota T, et al. (2009) CCL2 accelerates microglia-mediated Abeta oligomer formation and progression of neurocognitive dysfunction. *PLoS ONE* 4:e6197.
43. Hsiao K, et al. (1996) Correlative memory deficits, Abeta elevation, and amyloid plaques in transgenic mice. *Science* 274:99–102.
44. Martin BK, et al.; ADAPT Research Group (2008) Cognitive function over time in the Alzheimer's Disease Anti-inflammatory Prevention Trial (ADAPT): Results of a randomized, controlled trial of naproxen and celecoxib. *Arch Neurol* 65:896–905.
45. Shors TJ, et al. (2001) Neurogenesis in the adult is involved in the formation of trace memories. *Nature* 410:372–376.
46. Aimone JB, Wiles J, Gage FH (2009) Computational influence of adult neurogenesis on memory encoding. *Neuron* 61:187–202.
47. Yamasaki TR, et al. (2007) Neural stem cells improve memory in an inducible mouse model of neuronal loss. *J Neurosci* 27:11925–11933.
48. Donovan MH, et al. (2006) Decreased adult hippocampal neurogenesis in the PDAPP mouse model of Alzheimer's disease. *J Comp Neurol* 495:70–83.
49. Feng R, et al. (2001) Deficient neurogenesis in forebrain-specific presenilin-1 knockout mice is associated with reduced clearance of hippocampal memory traces. *Neuron* 32:911–926.
50. Haughey NJ, et al. (2002) Disruption of neurogenesis by amyloid beta-peptide, and perturbed neural progenitor cell homeostasis, in models of Alzheimer's disease. *J Neurochem* 83:1509–1524.
51. Wen PH, et al. (2004) The presenilin-1 familial Alzheimer disease mutant P117L impairs neurogenesis in the hippocampus of adult mice. *Exp Neurol* 188:224–237.
52. Jin K, et al. (2004) Enhanced neurogenesis in Alzheimer's disease transgenic (PDGF-APPSw,Ind) mice. *Proc Natl Acad Sci USA* 101:13363–13367.
53. Wang JM, et al. (2010) Allopregnanolone reverses neurogenic and cognitive deficits in mouse model of Alzheimer's disease. *Proc Natl Acad Sci USA* 107:6498–6503.
54. Magnus T, Chan A, Savill J, Toyka KV, Gold R (2002) Phagocytotic removal of apoptotic, inflammatory lymphocytes in the central nervous system by microglia and its functional implications. *J Neuroimmunol* 130:1–9.
55. Waldau B, Shetty AK (2008) Behavior of neural stem cells in the Alzheimer brain. *Cell Mol Life Sci* 65:2372–2384.
56. Qian X, Davis AA, Goderie SK, Temple S (1997) FGF2 concentration regulates the generation of neurons and glia from multipotent cortical stem cells. *Neuron* 18: 81–93.
57. Stachowiak MK, Maher PA, Joy A, Mordechai E, Stachowiak EK (1996) Nuclear localization of functional FGF receptor 1 in human astrocytes suggests a novel mechanism for growth factor action. *Brain Res Mol Brain Res* 38:161–165.
58. Stachowiak MK, Maher PA, Stachowiak EK (2007) Integrative nuclear signaling in cell development—a role for FGF receptor-1. *DNA Cell Biol* 26:811–826.
59. Dunham-Ems SM, et al. (2009) Fibroblast growth factor receptor-1 (FGFR1) nuclear dynamics reveal a novel mechanism in transcription control. *Mol Biol Cell* 20: 2401–2412.
60. Stachowiak EK, Fang X, Myers J, Dunham S, Stachowiak MK (2003) cAMP-induced differentiation of human neuronal progenitor cells is mediated by nuclear fibroblast growth factor receptor-1 (FGFR1). *J Neurochem* 84:1296–1312.
61. Duff K, et al. (1996) Increased amyloid-beta42(43) in brains of mice expressing mutant presenilin 1. *Nature* 383:710–713.
62. Klein RL, et al. (2002) Measurements of vector-derived neurotrophic factor and green fluorescent protein levels in the brain. *Methods* 28:286–292.
63. Xiao W, et al. (1999) Gene therapy vectors based on adeno-associated virus type 1. *J Virol* 73:3994–4003.
64. Xiao X, Li J, McCown TJ, Samulski RJ (1997) Gene transfer by adeno-associated virus vectors into the central nervous system. *Exp Neurol* 144:113–124.
65. Yamamoto M, et al. (2005) Overexpression of monocyte chemotactic protein-1/CCL2 in beta-amyloid precursor protein transgenic mice show accelerated diffuse beta-amyloid deposition. *Am J Pathol* 166:1475–1485.
66. Yamamoto M, et al. (2007) Interferon-gamma and tumor necrosis factor-alpha regulate amyloid-beta plaque deposition and beta-secretase expression in Swedish mutant APP transgenic mice. *Am J Pathol* 170:680–692.
67. Anderson ER, et al. (2003) Hippocampal synaptic dysfunction in a murine model of human immunodeficiency virus type 1 encephalitis. *Neuroscience* 118:359–369.

68. Anderson ER, Gendelman HE, Xiong H (2004) Memantine protects hippocampal neuronal function in murine human immunodeficiency virus type 1 encephalitis. *J Neurosci* 24:7194–7198.
69. Sato S, et al. (2008) Spatial learning impairment, enhanced CDK5/p35 activity, and downregulation of NMDA receptor expression in transgenic mice expressing tau-tubulin kinase 1. *J Neurosci* 28:14511–14521.
70. Lan X, et al. (2011) HIV-1 reduces Abeta-degrading enzymatic activities in primary human mononuclear phagocytes. *J Immunol* 186:6925–6932.
71. Xu J, et al. (2010) Actin interaction and regulation of cyclin-dependent kinase 5/p35 complex activity. *J Neurochem* 116:192–204.
72. Tokuraku K, Marquardt M, Ikezu T (2009) Real-time imaging and quantification of amyloid-beta peptide aggregates by novel quantum-dot nanoprobes. *PLoS ONE* 4:e8492.